CHAPTER 3

Development of Polyurethane (urethane-modified polyesteramide) Polymer using Mahua oil and Castor oil

3.1. Introduction

Polyurethane (PU), a highly versatile group within the polymer family, finds wide-ranging applications in various industries. The main benefit of PU polymer is the possibility of changing the molecular chain structure and managed the desire properties like elasticity, flexibility, and damping ability. It holds the position of the sixth most used polymer globally, making up approximately 8% of the total polymer market worldwide.[1–3] In 2016, the global production of PU amounted to 18 million tonnes, and it is projected that the global demand for PU will increase to 22.5 million tonnes by the year 2024.[4] In the past, PU was usually made through a process called "addition polymerization," which involves a reaction between the hydroxyl groups of polyol and the isocyanate functional groups of isocyanate.[5,6] The selection of specific isocyanate and polyol types used in the development of PU leads to the formation of PU in the rigid or flexible foam, coating, elastomer, adhesive, and thermoplastic form. Each form possesses unique characteristics that make it suitable for specific applications.[7] The most popular method for synthesising PU polymers is the step-growth polymerization of polyols produced from petrochemicals with various isocyanates.[8] The main problem accompanying with the use of petrochemical resources for the synthesis and development of PU polymers are environment pollution and waste disposal, high cost, and diminish of petroleum materials. Since isocyanates can be bought commercially and used to make PU, making renewable polyols has become an important area of research because they can be used to make PU in a sustainable way. The researchers are focusing on the utilisation of non-polluting and easy available renewable resources for preparing polyols for PU polymer synthesis.[9]

Vegetable oil (VO) as a renewable resource is an ideal candidate for polyol production to replace petrochemicals because of its vast abundance, high availability, cost-effectiveness, high biodegradability, and nontoxicity.[9–16] Many VOs have active sites (such as double bonds, ester linkages, hydroxyl, and α-methylene groups), which can be modified by many routes to produce different oleochemicals.[17–19] VOs are modified to add hydroxyl groups to their structures. This gives rise to polyols, which are essential for making PUs.[20] The modification of VOs through various reaction processes have been known.[16] On the contrary, food crisis problems often limit the utilisation of non-edible vegetable oils (EVOs) in industrial applications worldwide. However, many reports have shown the synthesis of polyols from different VOs such as cottonseed, canola, castor, cashew nut, jatropha, linseed, mahua, nahar, neem, soybean, and tobacco seed oils and their frequent use in the production

of PUs.[21–27] The utilisation of NEVOs to obtain valuable products reduces the consumption of EVOs, which is the demand of today's chemical industries. Therefore, the search and assessment of the indigenous non-edible VOs is a promising approach in polymer synthesis.[28]

In this context, we are exploring mahua oil (MO) as a new, NEVO as a renewable resource for the PU synthesis. Because of the Mahua plant, belonging to the *Sapotaceae* family and known as the Indian butter tree, is found in various parts of India and its neighbouring regions. The seeds of the Mahua plant contain approximately 30%–40% non-edible oil, which is used as a polyol resource.[29] MO is categorized as a drying oil that can be used for the synthesis of polymeric materials such as alkyd resins and epoxies for coating applications.[30] Also, the important PU polymers in the pathways of MO-based fatty amide are converted into polyetheramide polyols through a condensation with bisphenol-A or its derivatives, which further treat with toluenediisocynate and methylenediphenyldiisocynate to form MO-based PU for excellent coating applications was reported by Pawar et al.[31] The prepared PU coatings was safely used up to 220°-230°C as anticorrosive protection.

Another one of the most explored non-edible oils is CO, extracted from the seeds of *Ricinus communis L.,* which is a promising renewable polyol for synthesis of PU polymers.[32,33] CO is primarily composed of the triglyceride of ricinoleic acid (12-hydroxy-*cis*-9-octadecenoic acid, 87–90%), and its average hydroxy functionality is 2.7, which favours its use in PU synthesis.[34]

In the present work, we synthesized mahua fattyamide (MFA) using MO and diethanolamine, which is reacted with itaconic acid to produce polyesteramide (PEA). Here, we used itaconic acid (IA) because it is a natural compound that is non-toxic and easily degradable through natural processes. It finds extensive application in the creation of various polymers.[35] Using the various compositions of synthesized PEA and CO with isophorondiisocyanate (IPDI), different urethane-modified polyesteramides (UmPEA) polymers were developed. To the finding in our literature, such routes of PU synthesis have not been reported yet. There are no works (similar studies) about PU development using the combination of mahua oil-based polyols with castor oil. The synthesized MFA, PEA, and UmPEAs are well characterized using spectroscopic techniques. The physico-chemical properties like acid value, saponification value, iodine value, and hydroxyl value were determined using ASTM methods. The swelling behavior of synthesized UmPEA films was checked in ethanol solvent for up to 48 hr. The chemical resistance performance of UmPEA films was assessed against water, acid, alkali, salt, and organic solvents using the immersion method. The thermal stability of the prepared UmPEA films was investigated through TGA

and DSC analyses. The kinetic parameters of UmPEA polymers were calculated using the Kissinger method. Finally, the morphologies of the synthesized UmPEA films were analyzed using the SEM technique. The present work proves that the newly synthesized UmPEA films will be helpful as anticorrosive coatings.

3.2. Experimental

3.2.1. Materials

Diethanolamine (DEA) (Merck; India), sodium methoxide (Merck; India), itaconic acid (CDH; India), Isophorone diisocyanate (IPDI, TCI; India), Dibutyltin dilaurate (DBTDL, TCI; India), were of analytical grade and used as such. All the other organic solvents used were of analytical grade and used with proper purification.

3.2.2. Methods

3.2.2.1. Synthesis of MFA

Figure 3.1 represents the synthesis process of MFA from MO as reported in the literature.[21] In this procedure, sodium methoxide (0.007 mol) and DEA (0.32 mol each) were added to the 500-mL RBF and heated, managing the temperature between 80°C to 90°C, for 25 min with agitation on a magnetic stirrer. The assembly was immersed in an oil bath after developing an inert atmosphere (through N_2 gas) with a specific set of temperature controllers. Over a period of 60–70 min, MO (0.1 mol, 87 gm) was gradually added to the reaction content, and the temperature was made gradually to 125°C. The entire reaction was kept at 125°C for another 4 hr with stirring. The reaction's completion was examined through solubility checking in methanol. The product's complete solubility in methanol confirms its formation.[36–38] The final product was dissolved in diethyl ether and washed with a 15% aqueous NaCl solution. Using a separating funnel, the aqueous layer was separated from the organic ether layer, which had the MFA in it. The solvent was then removed through evaporation using a rota-evaporator. The yield of the MFA was 89%. ATR-FTIR and NMR spectroscopy were both used to carry out structural characterizations.

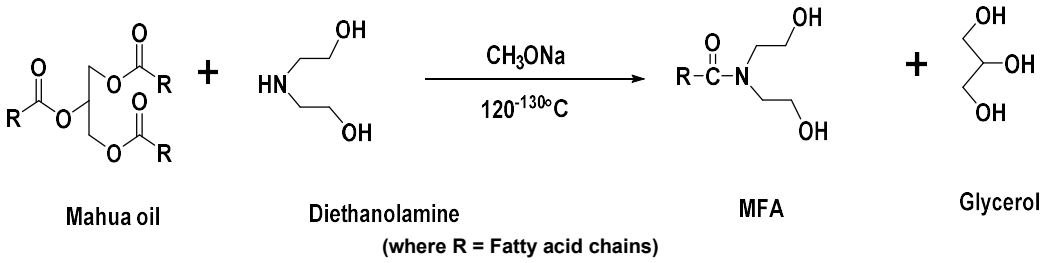

Figure 3.1. Synthesis of MFA

3.2.2.2. Synthesis of PEA

The reaction for the synthesis of PEA is given in **Figure 3.2**. MFA (0.20 mol) and itaconic acid (0.14 mol) were mixed in a solvent mixture (MEK (Methyl ethyl ketone) and xylene; 20:80) and placed in RBF (Round bottom flask). 2 to 3 drops of dilute H_2SO_4 as a catalyst are added. The reaction mixture was carried at 180°C for 3.5-4 hr with stirring. After managing an inert atmosphere (through N_2 gas), the vessel was dipped in an oil-bath with a proper arrangement of temperature controllers. The reaction was monitored until complete condensation of water occurred and was collected in a Dean-Stark apparatus trap. After finishing the reaction, the solvent was evaporated under reduced pressure in a rota-evaporator to obtain PEA resin.[19,39]

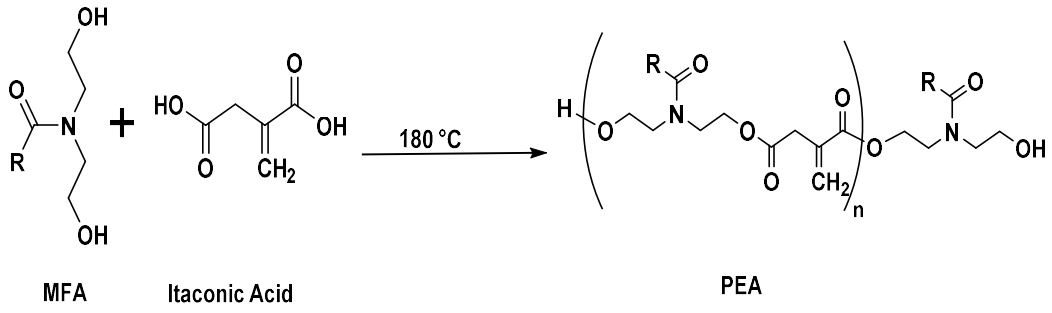

Figure 3.2. Synthesis of PEA

3.2.2.3 Synthesis of UmPEA

The UmPEA synthesis using PEA prepared as described above, CO, and IPDI is given in **Figure 3.3**. Using the different weight ratios of PEA and CO as polyols (shown in **Table 3.1**) with IPDI (40 wt%) and DBTDL catalyst (0.05 wt%) in MEK, they were put in RBF under an N_2 atmosphere. The reaction content was heated at 70°C for 2 hr with continuous stirring. The reaction was monitoring through the determination of hydroxyl value at regular interval.

Table 3.1. Chemical composition of polyols and IPDI for UmPEA resin formation

Polymer	PEA (gm)	Castor Oil (gm)	IPDI (gm)
UmPEA1	1.0	5.0	4.0
UmPEA2	2.0	4.0	4.0
UmPEA3	3.0	3.0	4.0
UmPEA4	4.0	2.0	4.0
UmPEA5	5.0	1.0	4.0

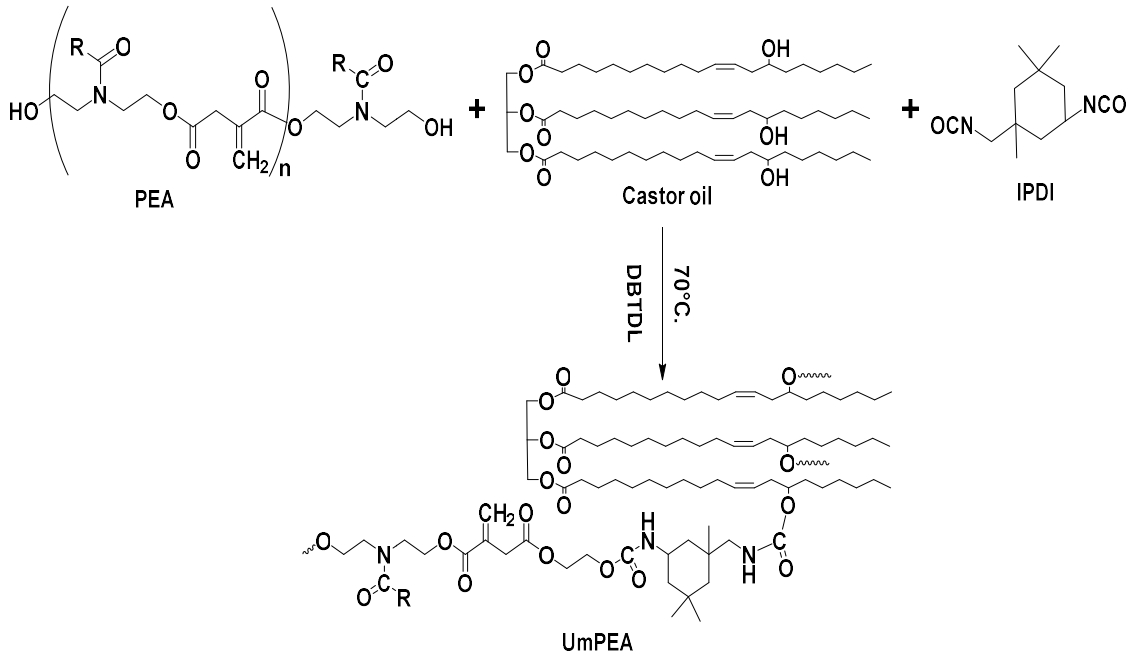

Figure 3.3. Synthesis of UmPEA

3.2.2.4. UmPEA film preparation

The solution cast method was employed to create UmPEA films using the silicon mold. The hot solution of UmPEA was placed in the silicon mold and allowed to dry at RT for almost 24 hr. The solid UmPEA films were obtained, and their thickness was found to be in the range of 0.87 to 0.89 mm, which is regulated through the adjustment of the volume of resin solution.

3.2.3. Characterization

The physico-chemical properties of MO, MFA, and PEA were characterized according to standard protocol methods for acid value (AV)(ASTM D5768-02), hydroxyl value (HV)(ASTM 1957-86), iodine value (IV)(ISI: 354, 1987), saponification value (SV)(ASTM D464-05), and specific gravity (SG)(ASTM D5355-95).

ATR-FTIR and ^{1}H NMR spectroscopic measurements were used to characterize the structure of MO, MFA, and PEA. ATR-FTIR spectra were measured in the range 4000-400 cm^{-1} on a Bruker Tensor 11 spectrometer. The spectrum of the air was taken as a background before sample analysis. The ATR-FTIR measurements were used to confirm the formation of UmPEA resins. ^{1}H NMR spectra were measured on 400 MHz Bruker Spectrometer by using tetramethylsilane (TMS) as an internal standard and $CDCl_3$ as a solvent.

The swelling behavior of UmPEA films was checked by immersing the small pieces (10 × 10 mm^2) of UmPEA samples into solvent (ethanol) at RT for up to 48 hr. Every regular

time interval of 2 hr, the weight of the samples was weighed after removing any excess solvent. The experiments were repeated three times for each sample, and the average value was considered. The swelling degree was determined using the gravimetric method.[40]

The chemical resistance (ASTM D1308) performances of UmPEA films were tested by dipping the films in an aqueous solution of NaOH (5%), HCl (5%), NaCl (5%), and toluene as organic solvent. The solvency resistance of UmPEA films was investigated by placing the film in various organic solvents for 24 hr at RT.

The glass transition temperature (Tg) of the UmPEA films was determined using DSC measurements conducted with TA Instruments (DSC 200 F3 Maia, NETZSCH-India). All DSC measurements were carried out using the standard ISO11357:1-2023 method. The measurements were performed in two cycles, in which the first cycle started from RT to -50°C, while the second cycle was performed in a temperature range of -50°C to 100°C with a heating rate of 10°C/min under a dry nitrogen atmosphere.

The TGA of UmPEA films with varying ratios was analyzed using a STA 449 F3 Jupiter analyzer from TA Instruments. The samples were subjected to heating from RT up to 700°C at different heating rates (10°, 15°, and 20°C/min). The experiment was conducted with nitrogen as the purge gas, and samples weighing less than 10 mg each were utilized for the test.

The morphologies of the UmPEA films were analysed by SEM using a JEOL JSM6300 (Japan) microscope operated at voltage acceleration of 10kV, magnification of 5000X and working distance of 15 nm.

3.3. Results and discussion

3.3.1. Physico-chemical properties

In **Table 3.2**, the physico-chemical properties of MO, MFA, and PEA are listed, such as their AV, HV, IV, SV, and SG. As per the determined values of the MO, MFA, and PEA, it can be concluded that the physico-chemical properties matched the standard values reported in the literature.[21,30] The IV of MO decreased in the synthesized PEA, which showed fewer double bonds. The HV of the PEA was 129 mg KOH/g, which was prompt to polymerize with isocyanate. PEA has higher molecular weights compared to MFA, resulting in an increased SG.

Table 3.2. Physico-chemical properties

Properties	MO	MFA	PEA
Appearance	Yellowish liquid	Yellow brown viscous liquid	Reddish brown viscous liquid
Acid value (mgKOH/gm)	8.33	2.46	12.17
Hydroxyl value (mgKOH/gm)	-	214.19	129.10
Iodine value (mgI_2/100gm)	63.78	59.56	55.23
Saponification value	196.59	-	-
Specific gravity @30°C	0.892	0.905	0.919

3.3.2. Structural Analysis

3.3.2.1. ATR-FTIR

Figure 3.4 shows the ATR-FTIR spectra of MO, MFA, and PEA, respectively. MO showed an absorption band at 1742 cm^{-1} due to the –C=O stretching of the ester group.[31] The spectrum of MFA showed a broad absorbance band at 3380 cm^{-1} for OH stretching of hydroxyl groups. The characteristic band at 1619 cm^{-1} is assigned to the C=O stretching of the carbonyl group present in MFA. The absorbance band at 1465 cm^{-1} is attributed to the C-N stretching of the amide linkage. The absence of amine functionality in diethanolamine in the spectra of MFA confirms its formation.[19] In the spectra of PEA, the absorption band of OH stretching of the hydroxyl group was found at 3,389 cm^{-1}. The stretching vibrations at 1358 cm^{-1} (–C-N) of amide linkage, 1632 cm^{-1} (–CON–) of amide carbonyl, and 1740 cm^{-1} (–COOR) of ester carbonyl groups are shown.[41] The total use of itaconic acid in the polyol formation is proven as the –COOH stretching vibration of itaconic acid was not found.[19]

The ATR-FTIR spectrum (**Figure 3.5**) of UmPEA films shows a prominent peak at 3393 cm^{-1} associated with the –NH stretching vibration of urethane linkages. All the films showed the stretching vibrations of the ester bond at 1710 cm^{-1}. The absorbance bands at 1646 cm^{-1} are for the amide carbonyl group –C=O and at 1480 cm^{-1} for –C-N, confirming the formation of UmPEA resins.

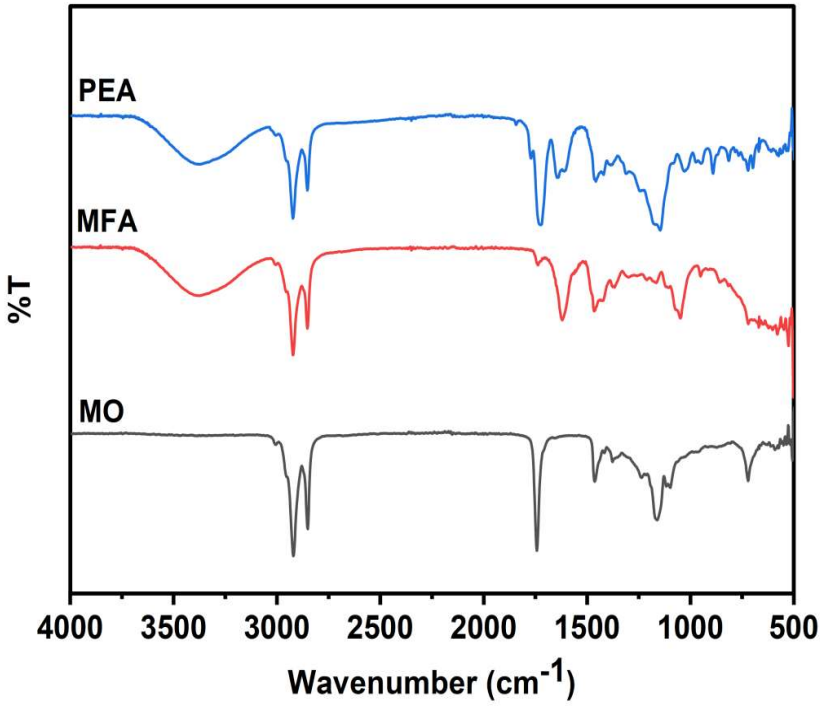

Figure 3.4. ATR-FTIR spectra of MO, MFA and PEA

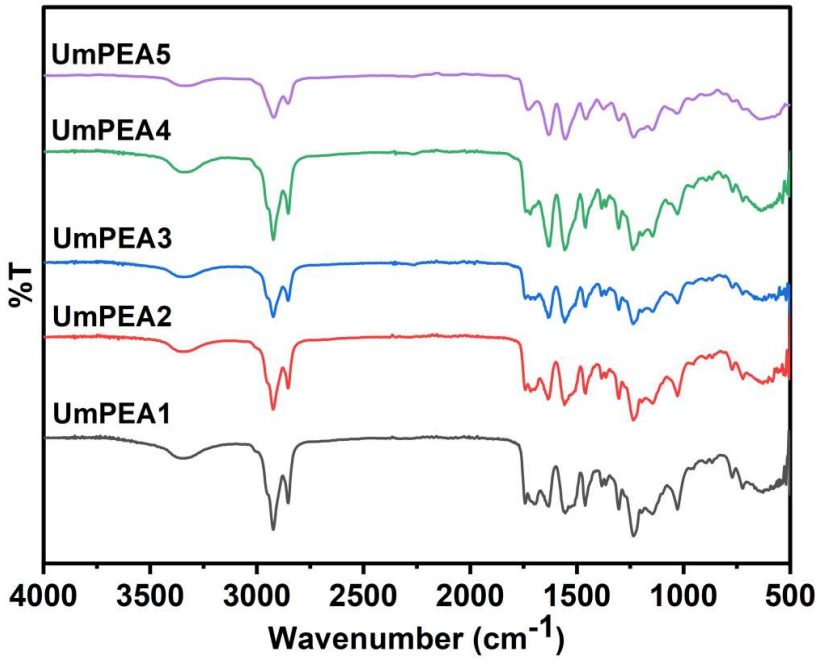

Figure 3.5. ATR-FTIR spectra of UmPEA films

3.3.2.2. ^{1}H NMR

Figure 3.6 displays the ^{1}H NMR spectra of MFA. The signal at δ 0.98 ppm corresponds to the terminal –CH_3 group of fatty acids, while signals recorded at δ 1.27 ppm

represent the proton of internal free $–CH_2$ groups present in the lengthy chains of fatty acids. The signals obtained at δ 1.91 ppm are due to $–CH_2$ group adjacent to the C=C bonds. The signal for protons of carbon that are linked to the carbonyl group of amide ($–CH_2–CO–NR_2$) is found at δ 2.32 ppm, while that for hydroxyl group protons is displayed at δ 4.65 ppm. The signal at δ 3.56 ppm is for protons of carbon linked to the nitrogen of amide. The signal shown at δ 4.67 ppm is for protons of $–CH_2$ attached to the hydroxyl group. The peak is recorded at δ 5.34 ppm for protons of the -CH=CH– group present in the MFA.

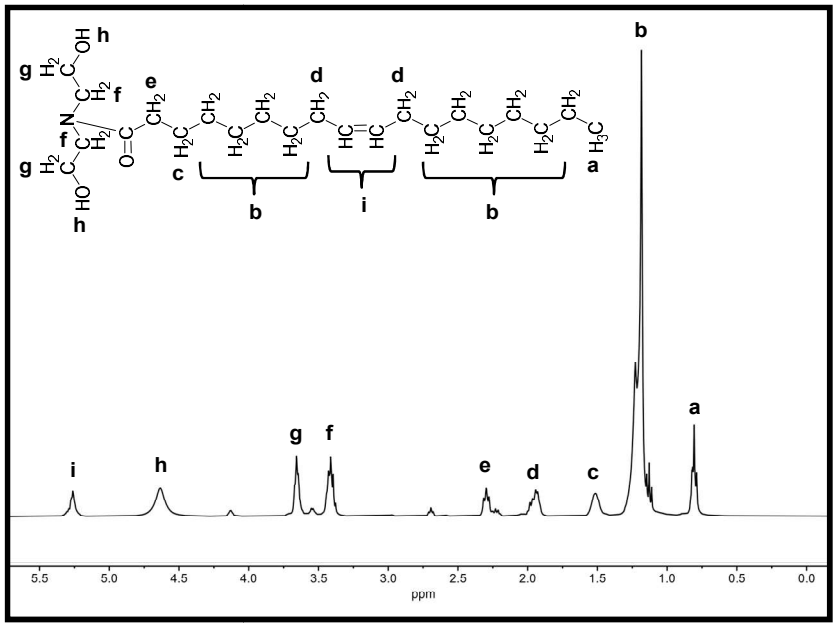

Figure 3.6. ^{1}H NMR Spectrum of MFA

The ^{1}H NMR spectrum of PEA is shown in **Figure 3.7**. The characteristic peak of terminal -CH_3 appears at δ 0.91 ppm. The internal fatty amide chain was observed at δ 1.28 ppm (–CH_2-). The signal appeared at δ 1.46 ppm, which corresponds to adjacent to $–CH_2$, which is connected to carbonyl amide group. The signal of the $–CH_2–$ group attached to the neighboring double bond was found at δ 2.07 ppm, whereas the peak appearance at δ 2.26 ppm was assigned to protons of the -CH_2- group attached to carbonyl functionality. The δ 3.36 ppm assigned to protons of the -CH_2- group bonded to amide nitrogen The proton of –CH_2– linked to the carbonyl group linked with oxygen is assigned to δ 4.31 ppm, and the peak at δ 4.83 ppm is related to the proton of the hydroxyl group. The proton detected at δ 5.54 ppm associated with unsaturated hydrocarbons (–CH=CH–) present in the fatty acid chain. The proton detected at δ 5.82 ppm and δ 6.55 ppm belongs to unsaturated CH_2 present in itaconic acid. Thus, the ^{1}H NMR spectrum clearly confirmed the formation of PEA.

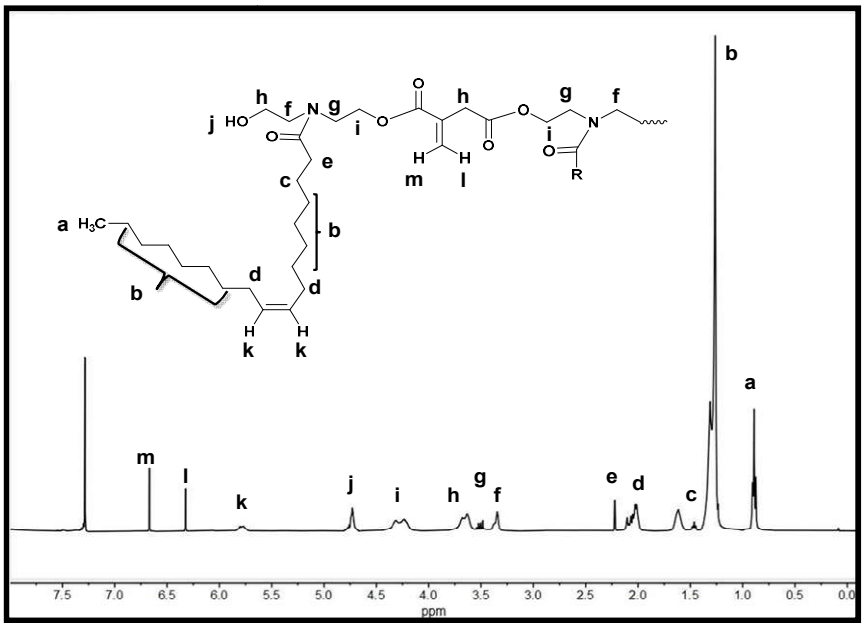

Figure 3.7. ^{1}H NMR Spectrum of PEA

3.3.3. Swelling behavior of UmPEA films

The swelling behavior of the synthesized UmPEA resin films was examined in ethanol. Swelling degree versus time for five UmPEA films composed of different weight ratios of polyols (PEA and CO) is presented in **Figure 3.8**.

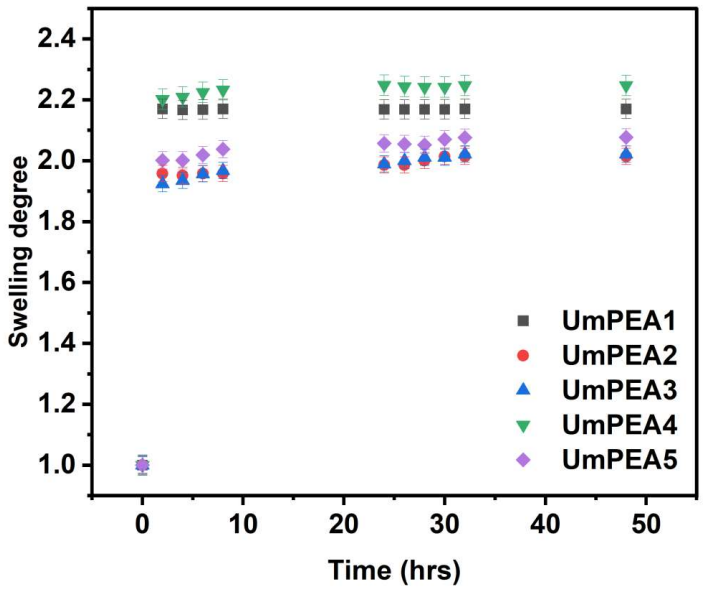

Figure 3.8. Swelling degree of the UmPEA films in ethanol versus time

It can be seen that all the samples increase in swelling degree with time and, after 2 hr, reach saturation. It indicates the stability of synthesized UmPEA films in common organic media, which favors their application as coating materials.

3.3.4. Chemical resistance performance of UmPEA films

By immersing the UmPEA film samples in distilled water, 5% NaOH (alkaline medium), 5% HCl (acidic medium), 5% NaCl (salt medium), and organic solvent, the visual changes that occurred in the samples were observed. The chemical resistance performance of all the UmPEA samples was observed and is shown in **Table 3.3** and their respective images before after processing is presented in **Figure 3.9**. From observations, it is clearly seen that the UmPEA1 performed well in the aqueous, alkaline, acidic, and salt mediums in comparison to the other four films. Not only that, UmPEA1 also loses a slight gloss in xylene solvent. All the UmPEA films remained unaffected in aqueous, alkaline, and acidic mediums, but UmPEA4 and UmPEA5 manifested dullness of gloss and slight film dissolution in salt solution (5% NaCl). Results clearly indicated that, due to the better stability of UmPEA films, which contain a higher content of CO, they resist better against the chemicals.[26] Of course, except for UmPEA1, all other films swelled when immersed in the xylene and lost their gloss totally. The chemical resistance provided by the films depends mainly on the relative inertness of the chemical structure and the degree of internal molecular cross-linking. Here, it was found that increasing the amount of CO in polyols in the UmPEA film formation effectively increased the cross-linking density of the film, which improved its stability and resistance against the salt and xylene medium.

Table 3.3. Chemical resistance performance of UmPEA films

Film/Property	Water resistance	Alkali resistance (5%NaOH)	Acid resistance (5%HCl)	Salt resistance (5%NaCl)	Solvent resistance (Xylene)
UmPEA1	A	a	a	a	b
UmPEA2	A	a	a	a	c
UmPEA3	A	a	a	a	c
UmPEA4	A	a	a	b	c
UmPEA5	A	a	a	b	c

a, *Not affected*; **b**, *slight loss in gloss*; **c**, *loss in gloss*

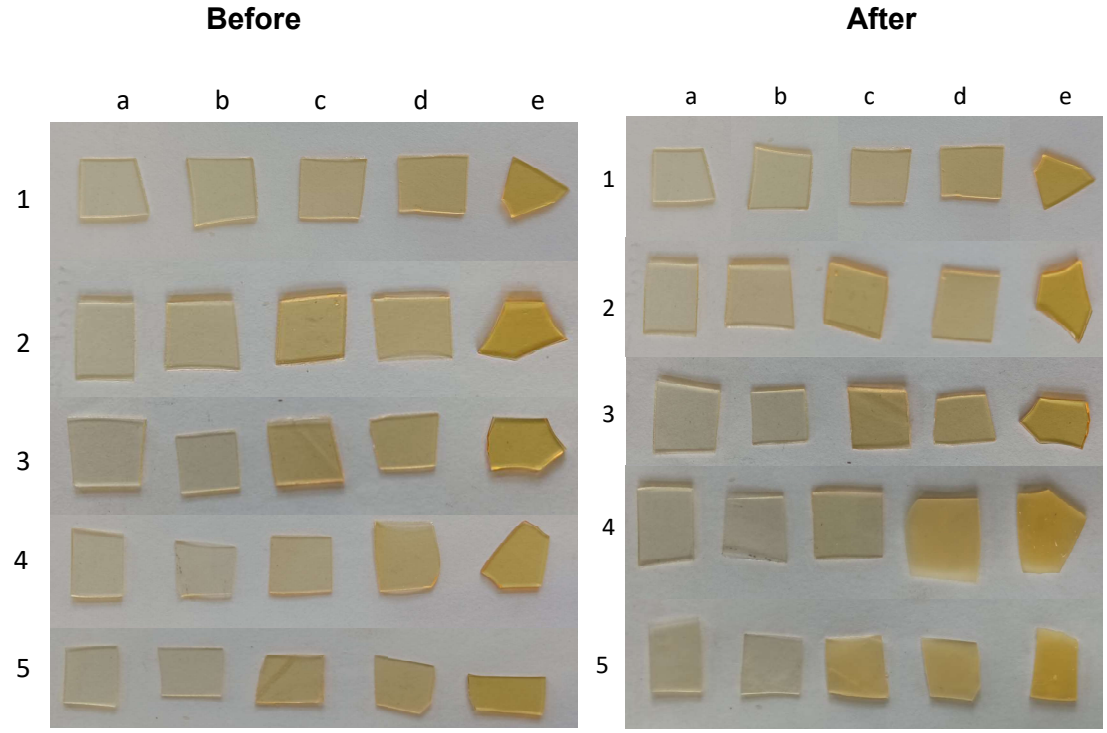

*The UmPEA films are coded as **a.** UmPEA1, **b.** UmPEA2, **c.** UmPEA3, **d.** UmPEA4, and **e.** UmPEA5*
*The chemical/media is numbered as **1.** Water, **2.** Alkali, **3.** Acid, **4.** Salt, **5.** Organic solvent*

Figure 3.9.UmPEA film images of before and after processing in various chemical media.

3.3.5. Solubility behavior of UmPEA films

The solubility behavior of the synthesized UmPEA films was checked through immersion techniques. The visual changes that occurred when UmPEA film was immerged in the various organic solvents are shown in **Table 4.4** their respective images before after processing is presented in **Figure 3.10**. The first three films (UmPEA1, UmPEA2, and UmPEA3) were insoluble at RT in all the studied organic solvents. In the case of UmPEA4, results showed it was slightly soluble in acetone and THF and remained undissolvable in other solvents. UmPEA5 was found insoluble in Chloroform, DMSO, and toluene and slightly soluble in all studied solvents. The solubility behavior of UmPEA films indicates that all developed films were capable of withstanding the material before breaking. Here, results clearly supported that when a higher amount of CO was taken with PEA in the UmPEA film formation, the films were found to have good insolubility in organic solvents.[42] As shown earlier, here too, increasing the amount of CO in polyols in the UmPEA film formation effectively increased the cross-linking density of the film, which improved its stability and resistance against most of the organic solvents.

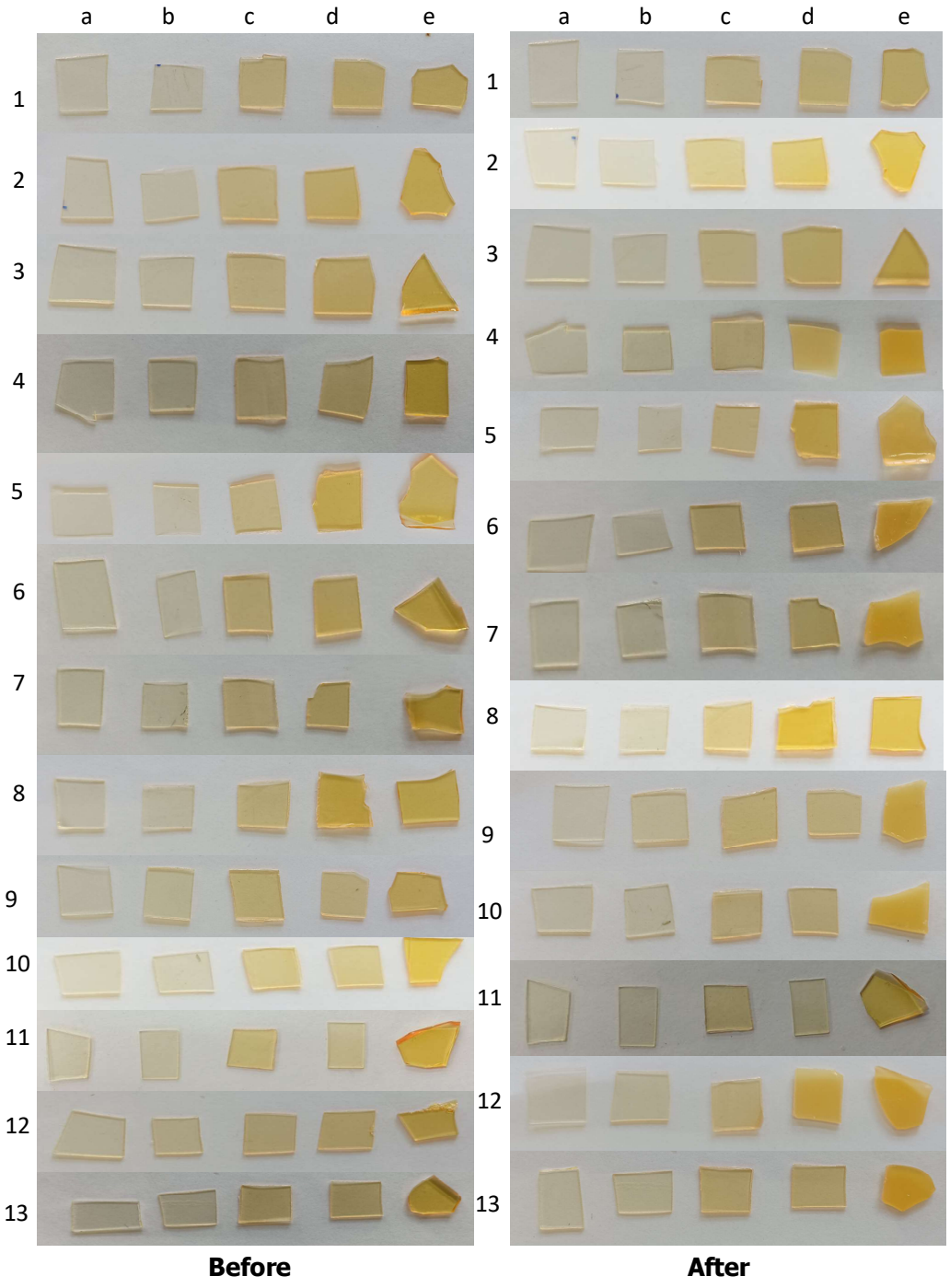

The UmPEA films are coded as a. UmPEA1, b. UmPEA2, c. UmPEA3, d. UmPEA4, and e. UmPEA5

The solvent is numbered as 1.Water, 2. Chloroform, 3. MEK, 4. Acetone, 5.Ethanol, 6.Methanol, 7. DCM, 8. DMSO, 9. DMF, 10. Ethyl acetate, 11. Toluene, 12. THF, 13. Chlorobenzene

Figure 3.10. UmPEA film images of before and after processing in various solvents.

Table 3.4. Solvent performance test of UmPEA films

Solvents/Films	UmPEA1	UmPEA2	UmPEA3	UmPEA4	UmPEA5
Water	- -	- -	- -	- -	- -
Chloroform	- -	- -	- -	- -	- -
MEK	- -	- -	- -	- -	+ -
Acetone	- -	- -	- -	+ -	+ -
Ethanol	- -	- -	- -	- -	+ -
Methanol	- -	- -	- -	- -	+ -
DCM	- -	- -	- -	- -	+ -
DMSO	- -	- -	- -	- -	- -
DMF	- -	- -	- -	- -	+ -
Ethyl acetate	- -	- -	- -	- -	+ -
Toluene	- -	- -	- -	- -	- -
THF	- -	- -	- -	+ -	+ -
Chlorobenzene	- -	- -	- -	- -	+ -

(++) soluble at RT; (+ -) slightly soluble at RT; (- -) insoluble at RT. MEK, methyethy ketone; DCM, dichloromethane; DMSO, dimethyl sulfoxide; DMF, N, N-dimethylformamide; THF, tetrahydrofuran.

3.3.6. Thermal Analysis

3.3.6.1. DSC

DSC thermograms of UmPEA films are shown in **Figure 3.11**. The peaks from the second heating DSC curves were taken to establish the Tg values of the UmPEA films. The Tg is the measure of the movement of a chain segment and checks a polymer's thermal behavior. The Tg values of the UmPEA polymeric films are 69.1°C, 64.9°C, 61.2°C, 59.1 °C, and 56.1°C for UmPEA1, UmPEA2, UmPEA3, UmPEA4, and UmPEA5, respectively. Results clearly indicated that the Tg of the polymer is higher with a higher content of CO in the composition. The influence on Tg is correlated with crosslink density, which relies on polymer functionality. Compared with other polyols, UmPEA films derived from CO showed the highest Tg value owing to their high crosslinking density and extra rigidity due to the presence of additional hydroxyl groups.[19] Therefore, an increase in Tg may be considered to the higher extent of cross-linking found with a higher CO content in UmPEA resin. Of course, the enhanced crosslink density decreases the chain segment mobility and energy (heat) required for molecular segments to achieve a smooth region.[43]

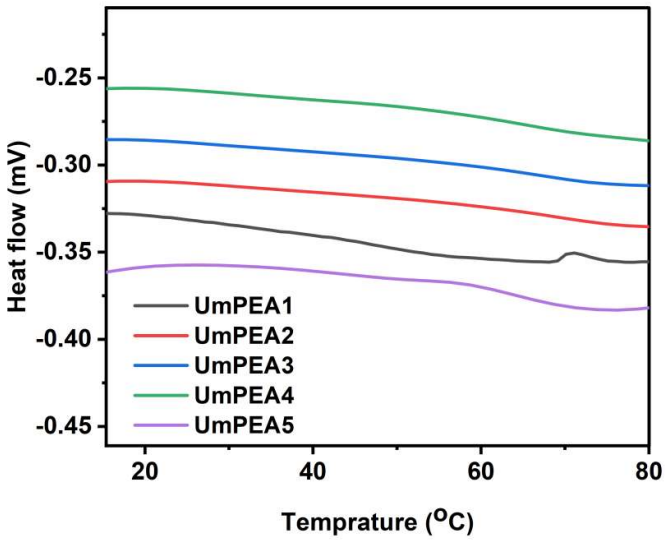

Figure 3.11. DSC curves of UmPEA films

3.3.6.2. TGA

The stability of PU polymers in thermal condition mainly depended on the structure of polyol (soft segment) and isocynate (hard segment). The TG curve of the UmPEA films at various heating rates (10°C/min, 15°C/min, and 20°C/min) and their derivative plots are presented in **Figure 3.12**. Generally, PU films exhibit low thermal stability, mainly due to the presence of labile urethane bonds. PU films tend to decompose at temperatures below 250 °C, depending on the types of isocyanates and polyols used during synthesis.[44] Upon analyzing the thermograms, it is seen that all the UmPEA films initiated degrading above 200 °C. The decomposition process up to 350°C can be attributed to the urethane bonds breaking, accompanied by the release of carbon dioxide.[45] Additionally, the range between 350° and 500°C temperature primarily corresponds to the degradation of the long alkyl chains present in the polyol segments. Also, thermal-oxidative break down of the UmPEA film takes place at temperatures morethan 500 °C. The increasing content of CO in the formation of UmPEA films enhances their thermal stability due to the high cross-linking density, which occurs through the inherent hydroxyl groups of CO.[19] The temperatures of the two stages of degradation of UmPEA films at different heating rates are given in **Table 3.5**.

Table 3.5. TGA data for UmPEA films

Sample	Tp_1 at different heating rates			Tp_2 at different heating rates		
	10°C/min	15°C/min	20°C/min	10°C/min	15°C/min	20°C/min
UmPEA1	353	359	355	463	467	462
UmPEA2	351	355	347	461	462	456
UmPEA3	353	354	340	450	450	443
UmPEA4	339	340	330	444	445	427
UmPEA5	330	331	332	435	431	439

As per **Table 3.5**, the maximum temperature at the 1st stage degradation (Tp_1) and 2nd stage degradation (Tp_2) values decrease with the decrease in the content of CO in UmPEA films for all the measured heating rates. Results clearly showed that with increasing heating rates, the Tp_1 and Tp_2 values first increase and then decrease with very small differences, which ultimately considered the similar thermal stability with the studied temperature for each individual UmPEA film. Hence, it is understood that the CO content in the UmPEA films plays a major role in the thermal behavior of the polymer, and its higher content provides thermal stability to the polymer. The improvement in stability in the UmPEA films is clearly observed by examining the T10, T50, and T95 values, which showed the 10, 50, and 95% weight loss of UmPEA films at different heating rates, respectively (displayed in **Tables 3.6, 3.7,** and **3.8**). The char residue of UmPEA1 to UmPEA5 films undergoes complete degradation at 700°C when the heating rate is 10°C/min. When the heating rate is increased to 15°C/min, the char residue decreases from 0.62% to 0.05% at 700°C. Similarly, at a heating rate of 20°C/min, the char residue decreases from 1.3% to 0.08% at 700°C.

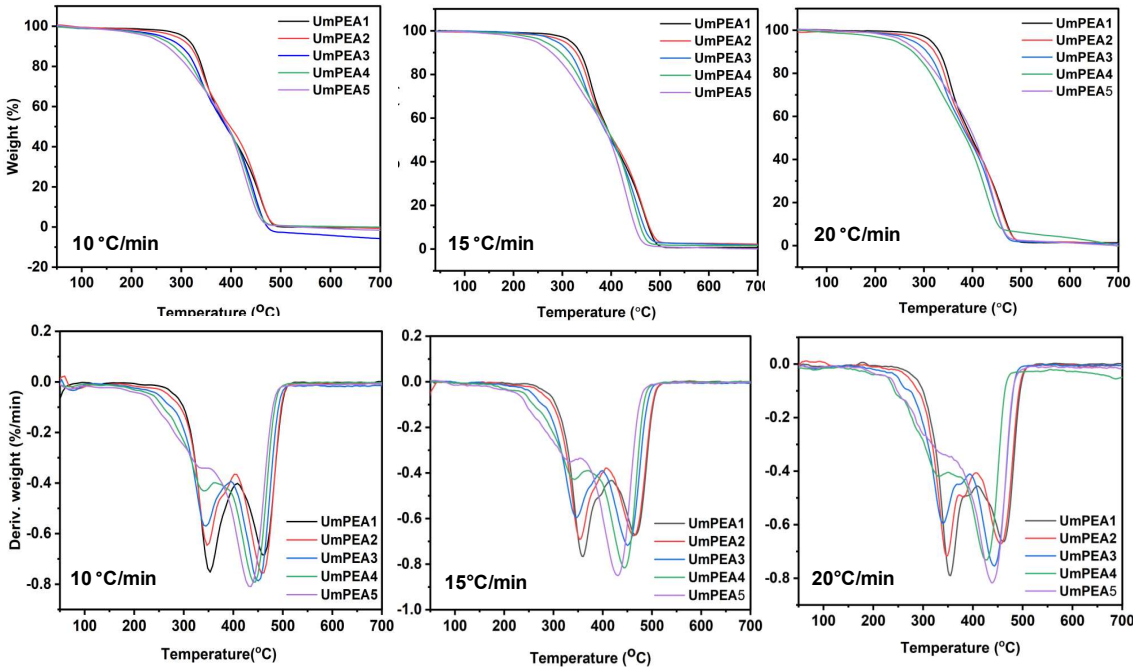

Figure 3.12. TGA curves and Derivative thermograms for the UmPEA films taken at various heating rates

Table 3.6. Thermal properties of UmPEA films at a heating rate of 10°C/min

Sample	Temperature(°C) at % weight loss			Char residue (%) at 700°C
	10%	50%	95%	
UmPEA1	284	374	457	00
UmPEA2	264	384	459	00
UmPEA3	244	384	454	00
UmPEA4	234	394	459	00
UmPEA5	229	399	459	00

Table 3.7. Thermal properties of UmPEA films at a heating rate of 15°C/min

Sample	Temperature (°C) at % weight loss			Char residue (%) at 700°C
	10%	50%	95%	
UmPEA1	298	387	470	0.62
UmPEA2	280	388	473	0.43
UmPEA3	275	392	472	0.28
UmPEA4	260	408	472	0.23
UmPEA5	242	405	465	0.05

Table 3.8. Thermal properties of UmPEA films at a heating rate of 20°C/min

Sample	Temperature(°C) at % weight loss			Char residue (%) at 700°C
	10%	50%	95%	
UmPEA1	306	392	476	1.34
UmPEA2	289	391	475	0.97
UmPEA3	277	400	475	0.88
UmPEA4	246	408	528	0.85
UmPEA5	260	413	478	0.08

"The Kissinger method was used to figure out the activation energy (Ea) parameters for the two different stages of the thermal decomposition process of UmPEA film. This involved utilizing the following equation to calculate the activation energy values[46]:

$$\ln\left(\frac{\beta}{Tp^2}\right) = -\frac{Ea}{RTp} + \{\ln\frac{AR}{Ea} + \ln[n(1-\alpha_P)^{n-1}]\} \qquad (1)$$

Here, the heating rate (β), the maximum temperature related to the maximum degradation (Tp), the pre-exponential factor (A), the activation energy (Ea), the maximum conversion (α_p), the order of the reaction (n), and the gas constant (R) are represented. The activation energy can be examined from the slope (=E_a/R) of a linear plot of ln(β/Tp^2) vs. 1/Tp.**"** [46]

The Ea measures for the UmPEA films were calculated and are provided in **Table 3.9** and their corresponding Kissinger plots (**Figure 3.13**) at two different degradation stages were presented. The kinetic parameters of films changed with the incorporation of CO. It was

observed that the Ea of the UmPEA film degradation process increased as the content of CO increased.

Table 3.9. Activation energy value of UmPEA films

Sample	Degradation (Tp_1)			Degradation(Tp_2)		
	Slope	R^2	E_a (kJ/mol)	Slope	R^2	E_a (kJ/mol)
UmPEA1	-26943.06	0.99938	224.00	-27211.19	0.99266	226.23
UmPEA2	-11359.86	0.99532	94.43	-24018.58	0.99416	199.68
UmPEA3	-604.59	1.00000	05.02	-14843.44	0.91952	123.40
UmPEA4	-595.15	0.99907	04.94	-13758.77	0.95522	144.38
UmPEA5	-519.29	0.99184	04.31	-12194.78	0.99223	101.38

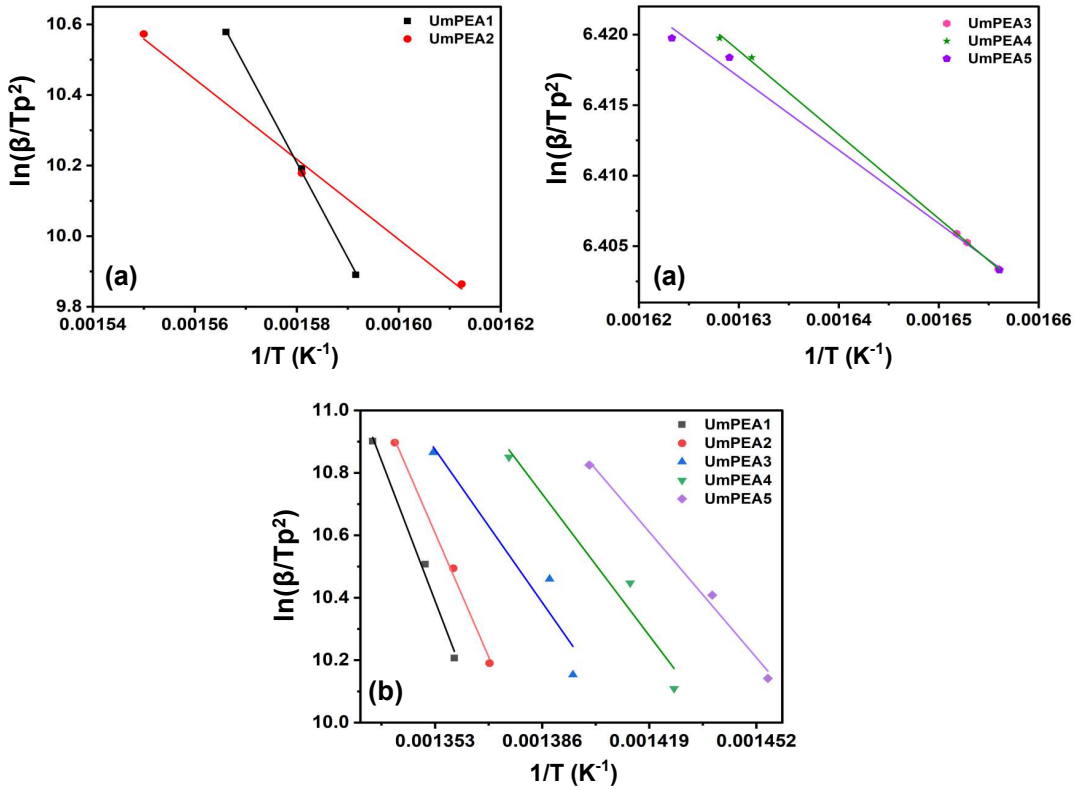

Figure 3.13. Kissinger plot of UmPEA films at two different stages of the degradation: (A) Tp_1 and (B) Tp_2.

The lowest CO content UmPEA5 film has the Ea values are 4.31 kJ mol^{-1} (Tp_1) and 101.38 kJ mol^{-1} (Tp_2), respectively. For higher CO content (5g) UmPEA1 film, the Ea values were measured to be 224 kJ mol^{-1} (Tp_1) and 226 kJ mol^{-1} (Tp_2), respectively, which were notable higher than other UmPEA films. This clearly demonstrates that an increase in the amount of CO in the UmPEA contributes to the higher thermal stability of the films. With the increase in activation energy, the thermal stability of the polymer was improved, and the

degradation became difficult, which showed that the flame retardancy of the polymer was improved. Also, the weight loss behavior of the UmPEA films at two different temperatures (360°C and 460°C) under various heating rates is provided in **Table 3.10**. From the data reported in Table 10, the decrease in the % decomposition of the film was shown with increasing the heating rate from 10°C/min to 20 °C/min, which demonstrated that the increasing heating rate was decreasing the thermal stability of the polymer. It was observed that the weight loss at both temperatures increased as the amount of CO increased. This indicates that the addition of CO enhances the thermal stability of the films due to better cross-linking occurring through the high hydroxyl groups of CO as the polyol.

Table 3.10. % Weight loss behavior for the UmPEA films

Sample	% decomposition up to 360 °C at different heating rates (°C/min)			% decomposition up to 470 °C at different heating rates (°C/min)		
	10	15	20	10	15	20
UmPEA1	41.98	36.06	32.97	94.64	88.96	86.11
UmPEA2	39.05	37.44	35.49	93.50	88.11	86.92
UmPEA3	39.63	35.61	31.58	96.60	88.56	85.12
UmPEA4	36.27	30.79	30.06	94.34	86.58	82.74
UmPEA5	34.66	31.11	28.32	94.44	89.49	83.54

3.3.7. Morphological analysis

SEM study was performed to find the morphological appearances of the prepared PU films. In **Figure 3.14**, the SEM images of UmPEA1, UmPEA2, and UmPEA3 films showed a homogenous phase and smooth surface. This clearly suggested that the flexible (PEA and CO) and rigid segments (diisocyanate) were distributed properly, resulting in good phase mixing morphology in the resins. Of course, these films are obtained with a high content of CO, which favors better phase mixing. The images of UmPEA4 and UmPEA5 films showed a rough surface due to the agglomerations. These results suggest poor interaction between the flexible and rigid segments of the film, as they were prepared with a lower content of CO.[42,47,48]

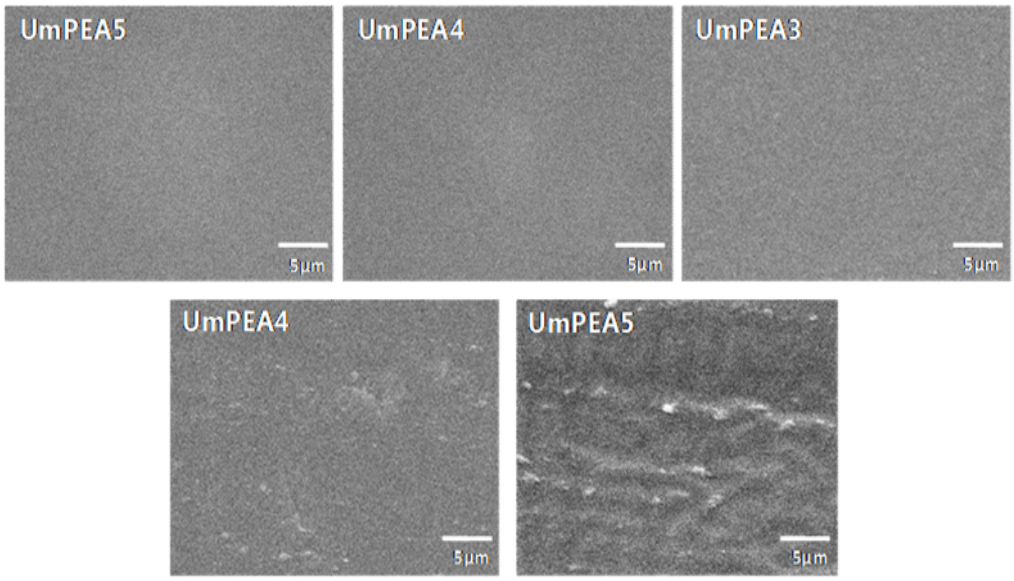

Figure 3.14. SEM images of UmPEA films.

3.4. References

(1) Kemona, A.; Piotrowska, M. Polyurethane recycling and disposal: methods and prospects. *Polymers* **2020**, *12* (8), 1752. https://doi.org/10.3390/polym12081752.

(2) Skoczinski, P.; Krause, L.; Raschka, A.; Dammer, L.; Carus, M. Current status and future development of plastics: solutions for a circular economy and limitations of environmental degradation. *Methods in Enzymology* **2021**, *648*, 1–26. https://doi.org/10.1016/bs.mie.2020.11.001.

(3) Błażek, K.; Datta, J. Renewable natural resources as green alternative substrates to obtain bio-based non-isocyanate polyurethanes-review. *Critical Reviews in Environmental Science and Technology* **2019**, *49* (3), 173–211. https://doi.org/10.1080/10643389.2018.1537741.

(4) Singh, I.; Samal, S. K.; Mohanty, S.; Nayak, S. K. Recent Advancement in Plant Oil Derived Polyol-Based Polyurethane Foam for Future Perspective: A review. *European Journal of Lipid Science and Technology* **2020**, *122* (3), 1900225. https://doi.org/10.1002/ejlt.201900225.

(5) Gama, N. V.; Ferreira, A.; Barros-Timmons, A. Polyurethane foams: past, present, and future. *Materials* **2018**, *11* (10), 1841. https://doi.org/10.3390/ma11101841.

(6) Ghasemlou, M.; Daver, F.; Ivanova, E. P.; Adhikari, B. Polyurethanes from seed oil-based polyols: a review of synthesis, mechanical and thermal properties. *Industrial Crops and Products* **2019**, *142*, 111841. https://doi.org/10.1016/j.indcrop.2019.111841.

(7) Tran, M. H.; Lee, E. Y. Production of polyols and polyurethane from biomass: A review. *Environmental Chemistry Letters* **2023**, *21* (4), 2199–2223. https://doi.org/10.1007/s10311-023-01592-4.

(8) Akindoyo, J. O.; Beg, M. D. H.; Ghazali, S.; Islam, M. R.; Jeyaratnam, N.; Yuvaraj, A. R. Polyurethane types, synthesis and applications – A review. *RSC Advances* **2016**, *6* (115), 114453–114482. https://doi.org/10.1039/C6RA14525F.

(9) Feng, Y.; Man, L.; Hu, Y.; Chen, L.; Xie, B.; Zhang, C.; Yuan, T.; Yang, Z. One-pot synthesis of polyurethane-imides with tailored performance from castor and tung oil. *Progress in Organic Coatings* **2019**, *132*, 62–69. https://doi.org/10.1016/j.porgcoat.2019.03.035.

(10) R. Meier, M. A.; O. Metzger, J.; S. Schubert, U. Plant oil renewable resources as green alternatives in polymer science. *Chemical Society Reviews* **2007**, *36* (11), 1788–1802. https://doi.org/10.1039/B703294C.

(11) Zhang, C.; Kessler, M. R. Bio-based polyurethane foam made from compatible blends of vegetable-oil-based polyol and petroleum-based polyol. *ACS Sustainable Chemistry & Engineering* **2015**, *3* (4), 743–749. https://doi.org/10.1021/acssuschemeng.5b00049.

(12) Thakur, V. K.; Thakur, M. K.; Raghavan, P.; Kessler, M. R. Progress in green polymer composites from lignin for multifunctional applications: A review. *ACS Sustainable Chemistry & Engineering* **2014**, *2* (5), 1072–1092. https://doi.org/10.1021/sc500087z.

(13) Pillai, C. K. S. Challenges for natural monomers and polymers: novel design strategies and engineering to develop advanced polymers. *Designed Monomers and Polymers* **2010**, *13* (2), 87–121. https://doi.org/10.1163/138577210X12634696333190.

(14) Konwar, U.; Karak, N. Epoxy-modified mesua ferrea l. Seed-oil-based polyester/clay nanocomposites. *International Journal of Polymeric Materials and Polymeric Biomaterials* **2011**, *60* (10), 799–816. https://doi.org/10.1080/00914037.2010.551366.

(15) Fernandes, F. C.; Kirwan, K.; Lehane, D.; Coles, S. R. Epoxy resin blends and composites from waste vegetable oil. *European Polymer Journal* **2017**, *89*, 449–460. https://doi.org/10.1016/j.eurpolymj.2017.02.005.

(16) Kaikade, D. S.; Sabnis, A. S. Polyurethane foams from vegetable oil-based polyols: A review. *Polymer Bulletin* **2023**, *80* (3), 2239–2261. https://doi.org/10.1007/s00289-022-04155-9.

(17) Alam, M.; Akram, D.; Sharmin, E.; Zafar, F.; Ahmad, S. Vegetable oil based eco-friendly coating materials: A review article. *Arabian Journal of Chemistry* **2014**, *7* (4), 469–479. https://doi.org/10.1016/j.arabjc.2013.12.023.

(18) Garrison, T. F.; Kessler, M. R.; Larock, R. C. Effects of unsaturation and different ring-opening methods on the properties of vegetable oil-based polyurethane coatings. *Polymer* **2014**, *55* (4), 1004–1011. https://doi.org/10.1016/j.polymer.2014.01.014.

(19) Paraskar, P. M.; Prabhudesai, M. S.; Kulkarni, R. D. Synthesis and characterizations of air-cured polyurethane coatings from vegetable oils and itaconic acid. *Reactive and Functional Polymers* **2020**, *156*, 104734. https://doi.org/10.1016/j.reactfunctpolym. 2020.104734.

(20) Kim, N.; Li, Y.; Sun, X. S. Epoxidation of camelina sativa oil and peel adhesion properties. *Industrial Crops and Products* **2015**, *64*, 1–8. https://doi.org/10.1016/ j.indcrop.2014.10.025.

(21) Chaudhari, A. B.; Anand, A.; Rajput, S. D.; Kulkarni, R. D.; Gite, V. V. Synthesis, characterization and application of azadirachta indica juss (neem oil) fatty amides (aijfa)

based polyurethanes coatings: A renewable novel approach. *Progress in Organic Coatings* **2013**, *76* (12), 1779–1785. https://doi.org/10.1016/j.porgcoat.2013.05.016.

(22) Gite, V. V.; Kulkarni, R. D.; Hundiwale, D. G.; Kapadi, U. R. Synthesis and characterisation of polyurethane coatings based on trimer of isophorone diisocyanate (ipdi) and monoglycerides of oils. *Surface Coatings International Part B: Coatings Transactions* **2006**, *89* (2), 117–122. https://doi.org/10.1007/BF02699641.

(23) Meshram, P. D.; Puri, R. G.; Patil, A. L.; Gite, V. V. Synthesis and characterization of modified cottonseed oil based polyesteramide for coating applications. *Progress in Organic Coatings* **2013**, *76* (9), 1144–1150. https://doi.org/10.1016/j.porgcoat. 2013.03.014.

(24) Gandhi, T. S.; Patel, M. R.; Dholakiya, B. Z. Synthesis and characterization of different types of epoxide-based mannich polyols from low-cost cashew nut shell liquid. *Research on Chemical Intermediate* **2014**, *40* (3), 1223–1232. https://doi.org/10.1007/ s11164-013-1034-2.

(25) Patel, K. I.; Parmar, R. J.; Parmar, J. S. Novel binder system for ultraviolet-curable coatings based on tobacco seed (nicotiana rustica) oil derivatives as a renewable resource. *Journal of Applied Polymer Science* **2008**, *107* (1), 71–81. https://doi.org/ 10.1002/app.27115.

(26) Mishra, V.; Mohanty, I.; Patel, M. R.; Patel, K. I. Development of green waterborne uv-curable castor oil-based urethane acrylate coatings: preparation and property analysis. *International Journal of Polymer Analysis and Characterization* **2015**, *20* (6), 504–513. https://doi.org/10.1080/1023666X.2015.1050852.

(27) Sharma, V.; Kundu, P. P. Condensation polymers from natural oils. *Progress in Polymer Science* **2008**, *33* (12), 1199–1215. https://doi.org/10.1016/j.progpolymsci. 2008.07.004.

(28) Raychura, A. J.; Dholakiya, B. Z.; Patel, K. I.; Jauhari, S. Development of non-traditional vegetable-oil-based two-pack polyurethane for wood-finished coating: an alternative approach. *ChemistrySelect* **2018**, *3* (39), 10837–10842. https://doi.org/ 10.1002/slct.201801452.

(29) Sarve, A. N.; Varma, M. N.; Sonawane, S. S. Response surface optimization and artificial neural network modeling of biodiesel production from crude mahua (madhuca indica) oil under supercritical ethanol conditions using co2 as co-solvent. *RSC Advances* **2015**, *5* (85), 69702–69713. https://doi.org/10.1039/C5RA11911A.

(30) Ganvit, V. M.; Sharma, R. K. Recent developments of madhuca indica (mahua) oil-based polymers: A mini review. *Polymers from Renewable Resources* **2022**, *13* (1–2), 55–70. https://doi.org/10.1177/20412479221109909.

(31) Pawar, M. S.; Kadam, A. S.; Yemul, O. S. Development of polyetheramide based corrosion protective polyurethane coating from mahua oil. *Progress in Organic Coatings* **2015**, *89*, 143–149. https://doi.org/10.1016/j.porgcoat.2015.08.017.

(32) Morales-Cerrada, R.; Tavernier, R.; Caillol, S. Fully bio-based thermosetting polyurethanes from bio-based polyols and isocyanates. *Polymers* **2021**, *13* (8), 1255. https://doi.org/10.3390/polym13081255.

(33) Matsuda, S.; Shibita, A.; Shimasaki, T.; Teramoto, N.; Shibata, M. Toughening modification of polyester–urethane networks incorporating oligolactide and oligocaprolactone segments by utilizing castor oil as a core molecule. *Polymer Bulletin* **2019**, *76* (10), 5313–5332. https://doi.org/10.1007/s00289-018-2656-8.

(34) Teramoto, N.; Saitoh, Y.; Takahashi, A.; Shibata, M. Biodegradable polyurethane elastomers prepared from isocyanate-terminated poly(ethylene adipate), castor oil, and glycerol. *Journal of Applied Polymer Science* **2010**, *115* (6), 3199–3204. https://doi.org/10.1002/app.30019.

(35) Ranjha, N. M.; Mudassir, J.; Akhtar, N. Methyl methacrylate-co-itaconic acid (mma-co-ia) hydrogels for controlled drug delivery. *Journal of Sol-Gel Sciences and Technology* **2008**, *47* (1), 23–30. https://doi.org/10.1007/s10971-008-1750-z.

(36) Gaikwad, M. S.; Kusumkar, V. V.; Yemul, O. S.; Hundiwale, D. G.; Mahulikar, P. P. Eco-friendly waterborne coating from bio-based polyester amide resin. *Polymer Bulletin* **2019**, *76* (6), 2743–2763. https://doi.org/10.1007/s00289-018-2511-y.

(37) Chaudhari, A.; Gite, V.; Rajput, S.; Mahulikar, P.; Kulkarni, R. Development of eco-friendly polyurethane coatings based on neem oil polyetheramide. *Industrial Crops and Products* **2013**, *50*, 550–556. https://doi.org/10.1016/j.indcrop.2013.08.018.

(38) Raychura, A. J.; Jauhari, S.; Patel, K. I.; Dholakiya, B. Z. A renewable approach toward the development of mahua oil-based wood protective polyurethane coatings: synthesis and performance evaluation. *Journal of Applied Polymer Science* **2018**, *135* (38), 46722. https://doi.org/10.1002/app.46722.

(39) Alam, M.; Alandis, N. M. Microwave assisted synthesis of urethane modified polyesteramide coatings from jatropha seed oil. *Journal of Polymers and the Environment* **2011**, *19* (3), 784–792. https://doi.org/10.1007/s10924-011-0328-y.

(40) Džunuzović, J.; Pergal, M.; Jovanović, S. M.; Vodnik, V. Synthesis and swelling behavior of polyurethane networks based on hyperbranched polymer. *Hemijska industrija* **2011**, *65* (6), 637–644. https://doi.org/10.2298/HEMIND110902071D.

(41) Patil, C. K.; Rajput, S. D.; Marathe, R. J.; Kulkarni, R. D.; Phadnis, H.; Sohn, D.; Mahulikar, P. P.; Gite, V. V. Synthesis of bio-based polyurethane coatings from vegetable oil and dicarboxylic acids. *Progress in Organic Coatings* **2017**, *106*, 87–95. https://doi.org/10.1016/j.porgcoat.2016.11.024.

(42) Munir, M. A.; Badri, K. H.; Heng, L. Y.; Inayatullah, A.; Badrul, H. A.; Emelda, E.; Dwinta, E.; Kusumawardani, N.; Wulandari, A. S.; Aprilia, V.; Supriyono, R. B. Y. Design and synthesis of conducting polymer bio-based polyurethane produced from palm kernel oil. *International Journal of Polymer Science* **2022**, *2022*, e6815187. https://doi.org/10.1155/2022/6815187.

(43) Phalak, G.; Patil, D.; Vignesh, V.; Mhaske, S. Development of tri-functional biobased reactive diluent from ricinoleic acid for uv curable coating application. *Industrial Crops and Products* **2018**, *119*, 9–21. https://doi.org/10.1016/j.indcrop.2018.04.001.

(44) Xia, Y.; Larock, R. C. Preparation and properties of aqueous castor oil-based polyurethane–silica nanocomposite dispersions through a sol–gel process. *Macromolecular Rapid Communications* **2011**, *32* (17), 1331–1337. https://doi.org/10.1002/marc.201100203.

(45) Petrović, Z. S.; Yang, L.; Zlatanić, A.; Zhang, W.; Javni, I. Network structure and properties of polyurethanes from soybean oil. *Journal of Applied Polymer Science* **2007**, *105* (5), 2717–2727. https://doi.org/10.1002/app.26346.

(46) Li, J.; Tong, L.; Fang, Z.; Gu, A.; Xu, Z. Thermal degradation behavior of multi-walled carbon nanotubes/polyamide 6 composites. *Polymer Degradation and Stability* **2006**, *91* (9), 2046–2052. https://doi.org/10.1016/j.polymdegradstab.2006.02.001.

(47) Panda, S. S.; Panda, B. P.; Mohanty, S.; Nayak, S. K. The castor oil based water borne polyurethane dispersion; effect of -nco/oh content: synthesis, characterization and properties. *Green Processing and Synthesis* **2017**, *6* (3), 341–351. https://doi.org/10.1515/gps-2016-0144.

(48) Zhang, T.; Zhang, W.; Deng, Y.; Chu, Y.; Zhong, Y.; Wang, G.; Xiong, Y.; Liu, X.; Chen, L.; Li, H. Curcumin-based waterborne polyurethane-gelatin composite bioactive films for effective uv shielding and inhibition of oil oxidation. *Food Control* **2022**, *141*, 109199. https://doi.org/10.1016/j.foodcont.2022.109199.